Computational and Experimental Studies on the Thermolysis Mechanism of Zirconium and Hafnium Tetraalkyl Complexes. Difference between Titanium and Zirconium Complexes

Yun-Dong Wu,*,† Zhi-Hui Peng,† Kyle W. K. Chan,† Xiaozhan Liu,‡ Albert A. Tuinman,‡ and Ziling Xue*,‡

Department of Chemistry, The Hong Kong University of Science and Technology, Clear Water Bay, Kowloon, Hong Kong, and Department of Chemistry, University of Tennessee, Knoxville, Tennessee 37996-1600

Received July 13, 1998

The first reaction step in the thermolysis of zirconium and hafnium tetraalkyl complexes has been studied with ab initio molecular orbital calculations in comparison with that of the titanium tetraalkyl complexes (Wu, Y.-D.; Peng Z.-H.; Xue, Z. *J. Am. Chem. Soc.* **1996**, *118*, 9772). Several clear differences in geometry and reactivity between TiR_4 and ZrR_4 (HfR_4) are predicted: (1) While $TiMe_4$ is in a staggered conformation, $ZrMe_4$ and $HfMe_4$ are predicted to be in an eclipsed conformation; (2) the activation energy for the unimolecular methane elimination through intramolecular hydrogen abstraction is in the order $TiMe_4 \ll ZrMe_4 < HfMe_4$; (3) the activation energy for the bimolecular methane elimination through intermolecular hydrogen abstraction for the three systems is much lower than that of the unimolecular mechanism and is in the order $ZrMe_4 < HfMe_4 < TiMe_4$; (4) unimolecular α-hydrogen abstraction for Ti(n-Pr)Me_3 and Ti(CH_2CMe_3)$_4$ is more favorable than γ-hydrogen abstraction. However, the opposite is predicted for the Zr and Hf complexes. Chemical vapor deposition of ZrC from Zr(CH_2CMe_3)$_4$ and Zr(CD_2CMe_3)$_4$ has been studied. The major volatile products are neopentane and isobutene, which are in a ratio of about 2.3 in both reactions. In the case of Zr(CD_2CMe_3)$_4$, the molar ratios of neopentane-d_2/neopentane-d_3 and isobutene-d_2/isobutene-d_0 are about 4.9 and 1.52, respectively. These support a mechanism in which γ-hydrogen abstraction is the first step of thermolysis.

Introduction

Early transition metal carbides are of particular interest in material science for their very high hardness and exceptional inertness to chemical attack.[1] In recent years, organometallic chemical vapor deposition (OMCVD) has been widely used in growing high-quality thin films at low temperatures,[2] and several transition metal carbides have been successfully prepared using metal alkyl complexes as the single precursor.[3−7]

Girolami et al. pioneered the low-temperature OMCVD of titanium carbide from tetraneopentyltitanium ($TiNp_4$) at 150 °C and conducted thorough studies of the mechanistic pathways in the thermolysis of $TiNp_4$.[3] The electron diffraction studies of the films showed the characteristic of an amorphous solid, while Auger electron spectroscopy (AES) revealed the Ti/C ratio of about 1:0.93, with little hydrogen content. Later, Smith et al. also carried out studies on the OMCVD of TiC, ZrC, and HfC from tetraneopentyl complexes.[4] They found that deposition temperatures above 500 °C are required to obtain stable crystalline thin films. A constant metal-to-carbon ratio of about 1:2 is observed by an AES depth profile under Smith et al.'s conditions. In addition, a large amount of hydrogen (up to 16%) was present in the films.[4] These results imply that different thermolysis mechanisms might be involved with different reaction conditions.

It has been known for a long time that the reactivity of MR_4 (M = Ti, Zr, Hf) complexes strongly depends on

† The Hong Kong University of Science and Technology.
‡ University of Tennessee.

(1) (a) Storms, E. K. *The Refractory Carbides*; Academic: New York, 1967; p 3. (b) Toth, L. E. *Transition Metal Carbides and Nitrides*; Academic: New York, 1971; p 141. (c) Zhang, N.; Wang, Y. *Thin Solid Films* **1992**, *214*, 4. (d) Schmickler, W.; Schultze, J. W. *Ber. Bunsen-Ges. Phys. Chem.* **1992**, *96*, 760.

(2) (a) Weiller, B. H. *J. Am. Chem. Soc.* **1996**, *118*, 4975. (b) Neumayer, D. A.; Ekerdt, J. G. *Chem. Mater.* **1996**, *8*, 9. (c) Zinn, A.; Niemer, B.; Kaesz, H. D. *Adv. Mater.* **1992**, *4*, 375. (d) MacInnes, A. N.; Power, M. B.; Hepp, A. F.; Barron, A. R. *J. Organomet. Chem.* **1993**, *449*, 95. (e) Maury, F. *Adv. Mater.* **1991**, *3*, 542.

(3) (a) Girolami, G. S.; Jesen, J. A.; Pollina, D. M.; Williams, W. S.; Kaloyeros, A. E.; Allocca, C. M. *J. Am. Chem. Soc.* **1987**, *109*, 1579. (b) Cheon, J.; Rogers, D. M.; Girolami, G. S. *J. Am. Chem. Soc.* **1997**, *119*, 6804. (c) Cheon, J.; Dubios, L. H.; Girolami, G. S. *J. Am. Chem. Soc.* **1997**, *119*, 6814.

(4) (a) Smith, D. C.; Rubiano, R. R.; Healy, M. D.; Springer, R. W. *Mater. Res. Soc. Symp. Proc.* **1993**, *282*, 643. (b) Smith, D. C.; Rubiano, R. R.; Healy, M. D.; Springer, R. W. *Proc. Twelfth Int. Symp. Chem. Vapor Deposition* **1993**, *93−2*, 417.

(5) Groshens, T. J.; Lowe-Ma, C. K.; Scheri, R. C.; Dalbey, R. Z. *Mater. Res. Soc. Symp. Proc.* **1993**, *282*, 299.

(6) Chisholm, M. H.; Caulton, K. G.; Xue, Z. *Chem. Mater.* **1991**, *3*, 384.

(7) (a) Healy, M. D.; Smith, D. C.; Rubiano, R. R.; Elliott, N. E.; Springer R. W. *Chem. Mater.* **1994**, *6*, 448. (b) Rutherford, N. M.; Larsen, C. E.; Jackson, R. L. *Mater. Res. Soc. Symp. Proc.* **1989**, *131*, 439. (c) Maury, F.; Ossola, F. *Thin Solid Films* **1992**, *207*, 82. (d) Maury, F.; Ossola, F. *Thin Solid Films* **1992**, *219*, 24.

10.1021/om980595v CCC: $18.00
Publication on Web 04/28/1999

Scheme 1

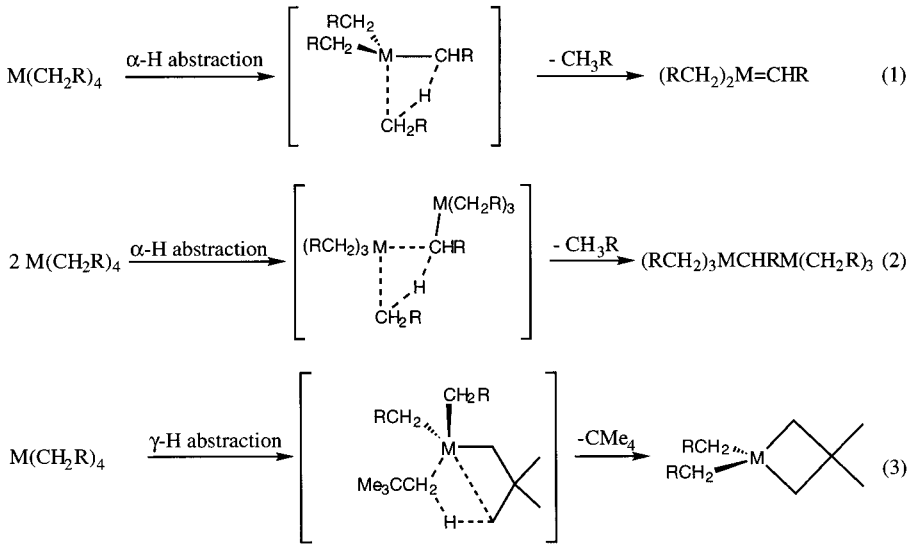

the steric effect and the metal itself.[8,9] Compounds MMe_4 are unstable. Thus, $TiMe_4$ thermolyzes under room temperature in ether to release CH_4 as the major organic product.[10] $ZrMe_4$ is less stable and thermolyzes even below −15 °C.[11] $HfMe_4$ has not been isolated. On the other hand, the MNp_4 (Np = neopentyl) compounds are much more stable. The stability increases in the order $TiNp_4 < ZrNp_4 < HfNp_4$. In benzene, the thermolysis conditions are as follows: $TiNp_4$, 60 °C ($t_{1/2}$ = 14.5 h); $ZrNp_4$, 80 °C ($t_{1/2}$ = 300 h); $HfNp_4$, 90 °C ($t_{1/2}$ = 900 h).[12] It is important to understand the thermolysis pathways of these transition-metal alkyl complexes to control their OMCVD processes. Three mechanisms of initial thermolysis are possible. As shown in Scheme 1, the first is through intramolecular α-hydrogen abstraction (eq 1), and the second is through intermolecular α-hydrogen abstraction (eq 2). Schrock et al. have postulated that when the alkyl group is small, e.g., methyl (R = H), the first step is the bimolecular intermolecular α-hydrogen abstraction (eq 2), which is the rate-determining step.[13,14] When the alkyl group becomes bulkier, the bimolecular mechanism becomes unfavorable because of steric reasons. But the unimolecular mechanism (eq 1) becomes feasible because of the release of steric interactions.[13] The third mechanism for the neopentyl complexes, a γ-hydrogen abstraction (eq 3) to form a metallacyclobutane, has been proposed and observed for several systems.[3,7c,15]

We have reported ab initio molecular orbital studies on the thermolysis of $NbMe_5$,[16] $TaMe_5$,[16] $TiMe_4$,[17] and $TiNp_4$.[17] Our calculations strongly support Schrock's hypothesis. As for the methyl complexes, the intermolecular (bimolecular mechanism) α-hydrogen abstraction has much lower activation energy than the intramolecular (unimolecular mechanism) α-hydrogen abstraction; the unimolecular α-hydrogen abstraction of $TiNp_4$ has a much lower activation energy than that of $TiMe_4$ because of the release of steric interactions in the former. Furthermore, the γ-hydrogen abstraction pathway for $TiNp_4$ has been found to have higher activation energy than the α-hydrogen abstraction pathway, which is also in line with the experiment.[18] Herein we report our further ab initio studies on the thermolysis of MMe_4, M(n-Pr)Me_3 (M = Zr, Hf), and $ZrNp_4$. We found that Zr and Hf complexes are quite different from Ti complexes in geometry, reactivity, and mode of thermolysis. We also report the experimental studies of thermolysis of $ZrNp_4$ in the CVD of ZrC. The results of these studies support the prediction by calculations.

Calculation Method and Experimental Section

All calculations were carried out with the GAUSSIAN 94 program.[19] For the $ZrMe_4$ and Zr(n-Pr)Me_3 system, geometries were fully optimized first with the Hartree−Fock method and

(8) (a) Davidson, P. J.; Lappert, M. F.; Pearce, R. *Chem. Rev.* **1976**, *76*, 219. (b) Schrock, R. R.; Parshall, G. W. *Chem. Rev.* **1976**, *76*, 243.
(9) (a) Bochmann, M. *Organometallics 1: Complexes With Transition Metal−Carbon σ-bonds*; Oxford: New York, 1994. (b) Yamamoto, A. *Organotransition Metal Chemistry: Fundamental Concepts and Applications*; John Wiley & Sons: New York, 1986; p 286.
(10) (a) Razuvaev, G. A.; Latyaeva, V. N.; Malysheva, A. V. *Pro. Acad. Sci. USSR* **1967**, *173*, 406. (b) D'yachkovskii, F. S.; Khrushch, N. E. *J. Gen. Chem. USSR* **1971**, *41*, 1787.
(11) Berthold, H. J.; Groh, G. *Angew. Chem., Int. Ed. Engl.* **1966**, *5*, 516.
(12) Davidson, P. J.; Lappert, M. F.; Pearce, R. *J. Organomet. Chem.* **1973**, *57*, 269.
(13) (a) Schrock, R. R. *Acc. Chem. Res.* **1979**, *12*, 98. (b) Shrock, R. R. *J. Organomet. Chem.* **1986**, *300*, 249.
(14) (a) Alt, H. G.; Di Sanza, F. P.; Ransch, M. D.; Uden, P. C. *J. Organomet. Chem.* **1976**, *107*, 257. (b) McDade, C.; Green, J. C.; Bercaw, J. E. *Organometallics* **1982**, *1*, 1629. (c) Bulls, A. R.; Schaefer, W. P.; Serfas, M.; Bercaw, J. E. *Organometallics* **1987**, *6*, 1219. (d) Heijden, H.; Hessen, B. *J. Chem. Soc., Chem. Commun.* **1995**, 145. (e) Andrés, R.; Gómez-Sal, P.; Jesús, E.; Martín, A.; Mena, M.; Yélamos, C. *Angew. Chem., Int. Ed. Engl.* **1997**, *36*, 115.
(15) Bruno, J. W.; Smith, G. M.; Marks, T. J.; Fair, C. K.; Schultz, A. J.; Willianms, J. M. *J. Am. Chem. Soc.* **1986**, *108*, 40, and references therein.
(16) Wu, Y.-D.; Chan, K. W. K.; Xue, Z. *J. Am. Chem. Soc.* **1995**, *117*, 9259.
(17) Wu, Y.-D.; Peng, Z.-H.; Xue, Z. *J. Am. Chem. Soc.* **1996**, *118*, 9772.
(18) Recently, Girolami et al. suggested that α-hydrogen abstraction is about 25 times faster than the γ-hydrogen abstraction based on isotopologue distribution in the thermolysis of $TiNp_4$-d_8 in deuterated benzene (C_6D_6). See ref 3b.
(19) Frisch, M. J.; Trucks, G. W.; Schlegel, H. B.; Gill, P. M. W.; Johnson, B. G.; Robb, M. A.; Cheeseman, J. R.; Keith, T. A.; Petersson, G. A.; Montgomery, J. A.; Raghavachari, K.; Al-Laham, M. A.; Zakrzewski, V. G.; Ortiz, J. V.; Foresman, J. B.; Cioslowski, J.; Stefanov B. B.; Nanayakkara, A.; Challacombe, M.; Peng, C. Y.; Ayala, P. Y.; Chen, W.; Wong M. W.; Andres J. L.; Replogle E. S.; Gomperts, R.; Martin R. L.; Fox, D. J.; Binkley, J. S.; Defrees, D. J.; Baker, J.; Stewart, J. P.; Head-Gordon, M.; Gonzalez, C.; Pople, J. A. *Gaussian 94*, Revision B.3; Gaussian, Inc.: Pittsburgh, PA, 1995.
(20) Dobbs, K. D.; Hehre, W. J. *J. Comput. Chem.* **1987**, *8*, 861.

the all-electron 3-21G basis set.[20] Harmonic vibration frequencies were calculated for each structure, based on which thermal energies and reaction entropy were calculated. The geometries were further optimized with the HW3 basis set according to Frenking's definition,[21] which was constructed by the contraction scheme {3311/2111/311] + effective core potential[22] on a 28-electron core for the zirconium atom and the 6-31G* basis set for carbon and hydrogen atoms. The energy of each structure was also calculated by the MP2/HW3 method on the HF/HW3 geometries. For the hafnium systems, since the 3-21G basis set for the hafnium atom is not available, geometry optimizations were performed with the HW3 basis set, [3311/2111/211] + ECP,[22] on a 60-electron core for the hafnium atom. This was followed by MP2/HW3 energy calculation. Vibration frequency calculations were not performed for the hafnium systems. Since the geometries of the hafnium systems are very similar to those of the corresponding zirconium systems, we have attempted to apply the vibration calculations for the zirconium systems to the hafnium systems. For the $ZrNp_4$ system, geometries were optimized with the HF/3-21G method, and thermal energies and reaction entropies were calculated on the basis of vibration frequencies with the HF/3-21G method.

All manipulations were performed under dry nitrogen or argon atmosphere with the use of either a glovebox or standard Schlenk techniques. Solvents were purified by distillation from potassium/benzophenone ketyl and stored under dry nitrogen. Benzene-d_6 was dried over activated molecular sieves and stored under N_2. $ZrBr_4$ (Aldrich) and $LiAlD_4$ (Aldrich, 98 at. % D, used for preparing Me_3CCD_2Br[23]) were used as received. Me_3CCD_2MgBr[23] and $Zr(CH_2CMe_3)_4$[12,24] were prepared by the literature methods. NMR spectra were recorded on a Bruker AC-250 or AMX-400 Fourier transform spectrometer; shifts were referenced to solvents (residual proton peak). CVD experiments with $ZrNp_4$-d_8 and $ZrNp_4$-d_0 were each performed twice, and the volatiles were analyzed.

Synthesis of $Zr(CD_2CMe_3)_4$. $ZrBr_4$ (0.840 g, 2.04 mmol) was slurried in 10 mL of Et_2O and cooled to −10 °C. Me_3CCD_2MgBr (0.195 M, 43 mL) was added dropwise at −10 °C with stirring. The solution was then stirred at 0 °C for 4 h and slowly warmed to room temperature overnight. Ether was removed under vacuum, and the product was extracted with hexanes. After filtration and removal of hexanes by vacuum, the solid was sublimed at 60 °C (0.01 Torr) to give 0.473 g (1.22 mmol, 60% yield) of the product. ^{1}H NMR (benzene-d_6, 250.1 MHz, 23 °C): δ 1.17 (CMe_3).

Dynamic Vacuum CVD.[4a] CVD was conducted in a horizontal, hot-wall CVD reactor at 400 °C with a base pressure of ca. 10^{-4}−10^{-5} Torr. A process similar to this has been used by Smith and co-workers to prepare ZrC thin films at 300−750 °C and 10^{-2}−10^{-4} Torr with either $Zr(CH_2CMe_3)_4$ or $Zr(CD_2CMe_3)_4$ as the precursor.[4a] The precursor was heated at 45 °C. Volatiles were collected in a liquid nitrogen trap downstream from the CVD reactor. After the deposition, the volatiles were transferred under vacuum to a J. Young valved NMR tube cooled to −196 °C. An internal standard, 4,4′-dimethylbiphenyl, was added to the NMR solvent, benzene-d_6, to measure the total carbon content in the volatiles. The procedures were repeated for the CVD using both $Zr(CH_2CMe_3)_4$ and $Zr(CD_2CMe_3)_4$ as the precursor.

The Analysis of Volatiles by NMR. The sample was first analyzed by ^{1}H (400.1 MHz) and ^{13}C (100.6 MHz) NMR before the analysis by MS. A correction was made for the presence of volatile samples in the "head space" in the NMR tubes using a procedure detailed by Girolami and co-workers.[3b] The ^{1}H and $^{13}C\{^1H\}$ NMR of the volatiles showed that the predominant organic products trapped were neopentane and isobutene isotopologues. Neopentane-d_2, $(H_3C)_3C-CHD_2$, was directly observed in the $^{13}C\{^1H\}$ NMR spectrum: $-CHD_2$ was identified as a 1:2:3:2:1 quintet at 31.21 ppm with an isotopic shift $^1\Delta$ of +0.60 ppm. Both isobutene-d_0 [^{1}H δ 4.71 (2H, $=CH_2$), 1.59 (6H, $=CMe_2$); $^{13}C\{^1H\}$ δ 141.90 ($=CMe_2$), 111.04 ($=CH_2$), 24.02 ($=CMe_2$)] and isobutene-d_2, $Me_2C=CD_2$, were identified in the ^{1}H and $^{13}C\{^1H\}$ NMR spectrum, although the peak of the $=CD_2$ in $(CH_3)_2C=CD_2$ as a triplet of triplet was not observed. The NMR isotopic shifts[25] for isobutene-d_2 were found: +2.4 ppb ($^4\Delta$) for CH_3, +0.10 ppm for CH_3 ($^3\Delta$), and +0.20 ppm for Me_2C ($^2\Delta$). A partially resolved triplet of triplets ($^3J_{D-C}$ = 1.9 Hz) assigned to the CH_3 in $(CH_3)_2C=CD_2$ was seen at 24.26 ppm in the $^{13}C\{^1H\}$ NMR spectrum. In addition, the ratio of integration of the CH_3 and $=CH_2$ groups is 7.3:1, rather than 3:1 as expected if only $(CH_3)_2C=CH_2$ is present. These observations are consistent with the presence of isobutene-d_2 as a volatile product in the CVD with $ZrNp_4$-d_8.

The Analysis of Volatiles by MS. Field-ionization mass spectrometry (FI-MS) was conducted on a VG ZAB-EQ hybrid high-performance spectrometer. The sample was introduced at ca. 10^{-7} atm. The emitter voltage was maintained at 6 kV, while the counter electrode was kept at 0 kV. Such +6 kV ionization voltage was found to minimize the fragmentation of neopentane. In the FI-MS spectrum of a neopentane-d_0 control sample, the intensity of mass 71 (M − 1) peak was found to be 0.8% of that of mass 72 (M) peak. In contrast, these two peaks were observed with ca. 50%:50% ratio by Hindennach and Block.[31a] In obtaining the ratios of the neopentane isotopologues, corrections were made for (1) the M − 1 peaks by using this ratio (0.8%) and (2) natural abundance ^{13}C isotopologues.

The volatiles from the CVD with $ZrNp_4$-d_8 were also analyzed by 70 eV electron-impact mass spectrometry. Girolami and co-workers have developed a method for the determination of the isotopic composition of samples of neopentane by electron-impact mass spectroscopy.[3b] Because neopentane does not give a parent peak in its 80 eV electron-impact mass spectrum, this method is based on the analysis of the intensities of the *tert*-butyl cations $(H_3C)_3C^+$, $(H_3C)_2(H_2DC)C^+$, $(H_3C)_2(HD_2C)C^+$, and $(H_3C)_2(D_3C)C^+$ at mass 57, 58, 59, and 60, respectively, as the products of neopentane ionization. However, in the current studies, the peaks of parent $(CH_3)_2C=CD_2$ and $(H_3C)_2(H_2DC)C^+$ overlap at mass 58. Thus this method could not be readily used for the quantitative analysis of the volatiles from the CVD with $ZrNp_4$-d_8, and the EI-MS data were not used in the calculations.

(21) (a) Jonas, V.; Frenking, G.; Reetz, M. T. *J. Comput. Chem.* **1992**, *13*, 919. (b) Jonas, V.; Frenking, G.; Reetz, M. T. *Organometallics* **1993,** *12*, 2111.
(22) Hay, P. J.; Wadt, W. R. *J. Chem. Phys.* **1985**, *82*, 299.
(23) Caulton, K. G.; Chisholm, M. H.; Streib, W. E.; Xue, Z. *J. Am. Chem. Soc.* **1991**, *113*, 6082.
(24) McAlexander L. H.; Li, L.; Yang, Y.; Pollitte, J. L.; Xue, Z. *Inorg. Chem.* **1998**, *37*, 1423.
(25) For a review on NMR isotopic shifts, see: Hansen, P. E. *Ann. Rep. NMR Spectrosc.* **1983**, *15*, 105.
(26) Cundari, T. R.; Li, Y. *Int. J. Quantum Chem.* **1995**, *55*, 315, and references therein.
(27) Pitzer, R. M. *Acc. Chem. Res.* **1983**, *16*, 207.
(28) (a) Hoffmann, R.; Jemmis, E.; Goddard, R. J. *J. Am. Chem. Soc.* **1980**, *102*, 7667. (b) Schultz, A. J.; Brown, R. K.; Williams, J. M.; Schrock, R. R. *J. Am. Chem. Soc.* **1981**, *103*, 169. (c) Brookhart, M.; Green, M. L. H.; Wong, L. L. *Prog. Inorg. Chem.* **1988**, *36*, 1. (d) Cummins, C. C.; van Duyne, G. D.; Schaller, C. P.; Wolczanski, P. T. *Organometallics* **1991**, *10*, 164. (e) Bai, Y.; Roesky, H.; Noltemeyer, M.; Witt, M. *Chem. Ber.* **1992**, *125*, 825.
(29) (a) Cundari, T. R.; Gordon, M. S. *J. Am. Chem. Soc.* **1993**, *115*, 4210. (b) Cundari, T. R. *J. Am. Chem. Soc.* **1992**, *104*, 1532.
(30) The calculated reaction energy of methane elimination from $HfMe_4$ is larger than the activation energy, which indicates the formation of the adduct between products. Cundari et al. have found the binding enthalpies of methane adducts of $(H)_2M=NH$ (M = Ti, Zr, Hf) to be about 9 kcal/mol; see ref 29a.
(31) (a) Cundari, T. R.; Gordon, M. S. *J. Am. Chem. Soc.* **1992**, *114*, 539. (b) Cundari, T. R.; Gordon, M. S. *J. Am. Chem. Soc.* **1991**, *113*, 5231.

Table 1. Calculated Changes of Energies (ΔE, kcal/mol), Thermal Energies ($\Delta\Delta H°_{298}$, kcal/mol), and Entropies (ΔS_{298}, cal/mol·K) for the Formation of Transition Structures and Products for Alkane Elimination from MMe_4, M(n-Pr)Me_3 (M = Zr, Hf), and $ZrNp_4$

		HF/3-21G			HF/HW3	MP2//HW3
entry	reaction	ΔE	$\Delta\Delta H°_{298}$	ΔS_{298}	ΔE	ΔE
1	(**1b**) → (**4b**)	66.8	−2.7	−4.8	69.7	51.2
2	(**1b**) → (**5b**) + CH_4	51.9	−1.4	35.4	48.9	48.5
3	(**1b**) + (**1b**) → (**6b**)	42.5	−0.1	−53.0	48.3	15.6
4	(**1b**) + (**1b**) → (**7b**) + CH_4	−11.3	0.6	−3.8	−10.5	−20.7
5	(**2b**) → (**8b**)	57.2	−3.2	−10.1	62.3	43.0
6	(**2b**) → (**9b**) + CH_4	14.3	−2.2	22.8	16.2	12.0
7	(**1c**) → (**4c**)				74.3	57.5
8	(**1c**) → (**5c**) + CH_4				58.8	60.2
9	(**1c**) + (**1c**) → (**6c**)				49.2	19.9
10	(**1c**) + (**1c**) → (**7c**) + CH_4				−10.9	−18.8
11	(**2c**) → (**8c**)				64.5	46.4
12	(**2c**) → (**9c**) + CH_4				16.6	13.0
13	(**3b**) → (**10b**)	61.5	−3.0	0.5		45.9[a]
14	(**3b**) → (**12b**)	54.3	−3.1	−3.9		40.1[b]
15	(**3b**) → (**11b**) + CMe_4	36.8	−1.8	37.6		33.4[c]
16	(**3b**) → (**13b**) + CMe_4	10.3	−2.4	36.2		8.0[d]

[a] Calculated on the basis of comparison with entry 1: 51.2 − (66.8−61.5). [b] Calculated on the basis of comparison with entry 5: 43.0 − (57.2−54.3). [c] Calculated on the basis of comparison with entry 2: 48.5 − (51.9−36.8). [d] Calculated on the basis of comparison with entry 6: 12.0 − (14.3−10.3).

Results and Discussion

The calculated total energies, thermal energies, and entropies of the reactants, transition structures, and the products of the reactions of $ZrMe_4$, Zr(n-Pr)Me_3, $HfMe_4$, Hf(n-Pr)Me_3, and $ZrNp_4$ are given in Table 1 of the Supporting Information. Table 1 gives the calculated reaction or activation energies, thermal energy ($T = 298$ K) corrections, and entropies of the thermolysis reactions.

A. Structures of the Reactants MMe_4 and M(n-Pr)Me_3 (M = Ti, Zr, Hf) and MNp_4 (M = Ti, Zr). Figure 1 shows the geometries of MMe_4 (**1**), MMe_3(n-Pr) (**2**) calculated with the HF/HW3 method, and MNp_4 (**3**) with the HF/3-21G method.

Two structures of MMe_4 (**1**), a staggered conformation with a dihedral angle H−C−M−C of 180° and an eclipsed conformation with a dihedral angle H−C−M−C of 0°, have been studied. With the MP2/HW3 method, the staggered conformation of $TiMe_4$ is more stable than the eclipsed conformation by about 2.2 kcal/mol,[17,21a] while the eclipsed conformation of $ZrMe_4$ and $HfMe_4$ is more stable than the staggered conformation by about 2.7 and 2.5 kcal/mol, respectively (see Figure 1). The HF/3-21G frequency calculation of $ZrMe_4$ shows that the eclipsed conformation is a true minimum, while the staggered conformation has four imaginary frequencies that correspond to the rotations of the methyl groups. Cundari's calculation on ZrH_3Me also showed an eclipsed conformation as a minimum.[26] The calculated Zr−C and Hf−C bond lengths are about 2.27 and 2.25 Å with the HF/HW3 method in both staggered and eclipsed conformations, with the Hf−C bond slightly shorter than the Zr−C bond. Both are longer than the Ti−C bond (2.08 Å)[17] by about 0.2 Å, which is in accord with their covalent radii: R_{Ti} (1.32 Å) < R_{Zr} (1.45 Å) ≈ R_{Hf} (1.44 Å).

The preference of eclipsed conformation for $ZrMe_4$ and $HfMe_4$ is interesting. We suspect that, because of the long length and large polarization of the Zr−C and Hf−C bonds, the closed-shell repulsion between C−H and Zr−C is not significant, which is often argued to be responsible for the preference for staggering.[27] Instead, the eclipsed conformation benefits from electrostatic and dispersion interactions between the partially negatively charged C and positively charged H atoms.

The methyl groups in Zr(n-Pr)Me_3 and Hf(n-Pr)Me_3 (**2b**, **2c**) are also in eclipsed conformations with respect to the M−C bonds, while in Ti(n-Pr)Me_3 (**2a**),[17] the methyl groups are in staggered conformations, which is similar to the situation in tetramethyl systems. However, the propyl group is in staggered conformation with the M−C−C angles of about 117° for all the three compounds, presumably due to steric interactions.

The tetrahedral geometry of $ZrNp_4$ (**3b**) is similar to its Ti analogue (**3a**), which has an S_4 symmetry. The Zr−C−C angle is about 123.2°, which is smaller than that of $TiNp_4$ by about 3°. Because the Zr−C bond length is longer than the Ti−C bond, $ZrNp_4$ is less crowded. The Zr−C−H angle is about 101°, indicating the existence of α-agostic effect.[28]

B. Thermolysis Reactions of MMe_4 and M(n-Pr)Me_3. Figure 2 shows the transition structures (**4**, **6**, **8**) and products (**5**, **7**, **9**) of the unimolecular and bimolecular α-hydrogen abstraction reactions for MMe_4 and γ-hydrogen abstraction reaction for M(n-Pr)Me_3 calculated with the HF/HW3 method. The calculated MP2/HW3 activation and reaction enthalpies (with HF/3-21G thermal energy corrections) for each reaction are also shown in Figure 2.

(1) Unimolecular α-Hydrogen Abstraction of MMe_4. The transition structures (TS) of $ZrMe_4$ (**4b**) and $HfMe_4$ (**4c**) are similar to that of $TiMe_4$ (**4a**),[17] which are in a kite-like shape with an obtuse angle about the H_t and three acute angles. As shown in Figure 2, the breaking C−H bonds are longer than that in the corresponding TS of $TiMe_4$ by about 0.04 Å (Zr) and 0.1 Å (Hf), while the forming C−H bonds are almost the same for $ZrMe_4$ (**4b**) and shorter by about 0.03 Å for $HfMe_4$ (**4c**), which indicates an even later transition structure. In addition, because of the longer breaking M−C and partially formed M═C bonds, the C−M−C

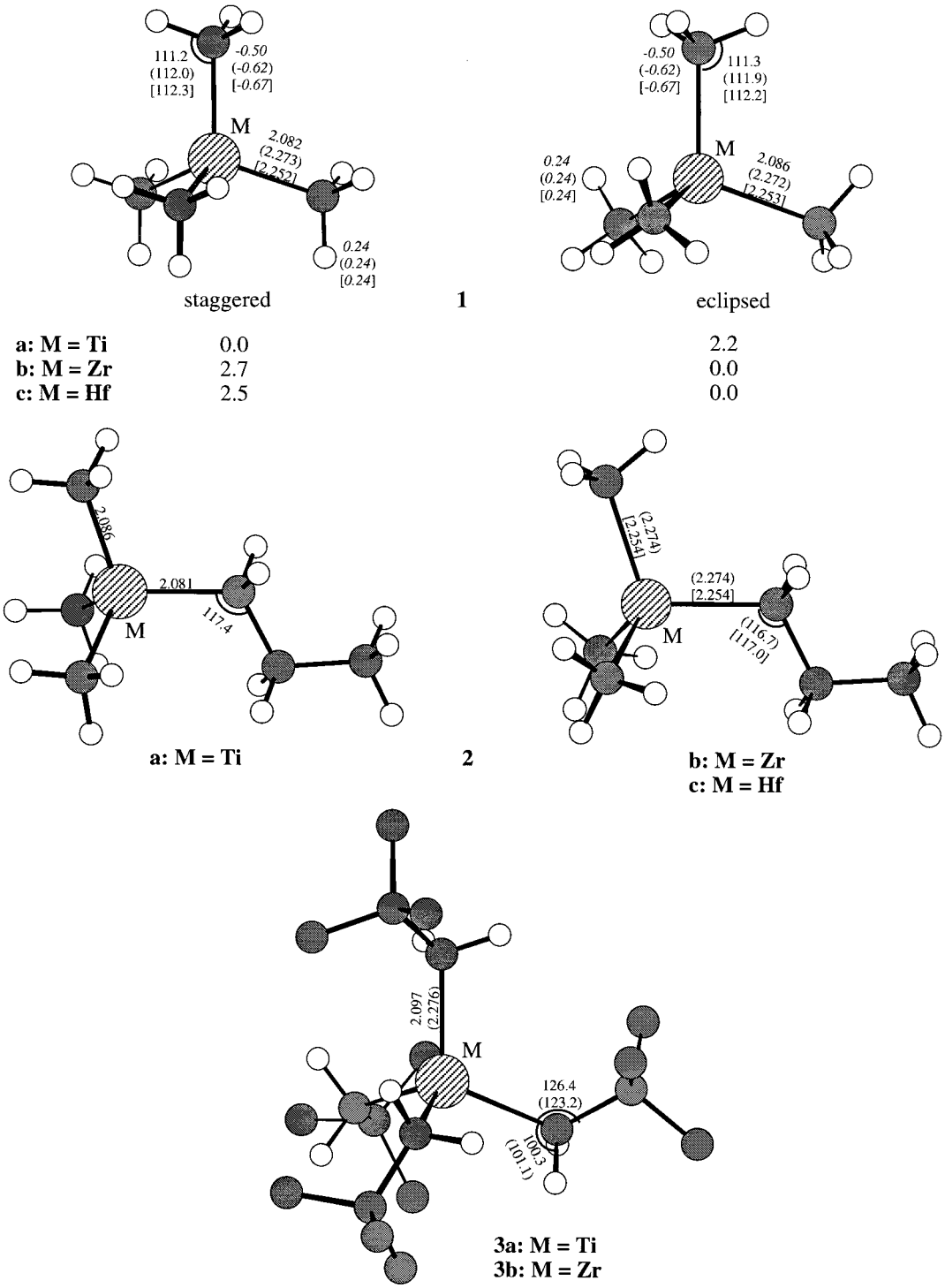

Figure 1. Calculated structures of MMe_4 (**1**) with the MP2/HW3 relative energies (kcal/mol) of the staggered and eclipsed conformations, M(n-Pr)Me_3 (**2**), and MNp_4 (**3**, with methyl hydrogens omitted for clarity). Selected geometrical parameters and NBO charges calculated with the HF/HW3 or Hf/3-21G methods are given for M = Ti (**a**), Zr (**b**, in parentheses), and Hf (**c**, in brackets).

bond angles are smaller (84.4° for $ZrMe_4$ and 86.1° for $HfMe_4$) than that in TS of $TiMe_4$ (91.4°).[17] The calculated activation enthalpies for the methane elimination of $ZrMe_4$ and $HfMe_4$ are 48.5 and 54.8 kcal/mol (see Figure 2 and Table 1, entries 1 and 7); the corresponding activation enthalpy for $TiMe_4$ is 38.6 kcal/mol.[17] Thus, we predict that the activation energy increases as the transition metal becomes heavier. Such a trend has also been found in Cundari et al.'s calculations for similar reactions.[26,29] This trend is due primarily to differences in the M−C bond energy. The mean bond dissociation energies for MNp_4 are D(Ti−C) = 44 kcal/mol, D(Zr−C) = 54 kcal/mol, and D(Hf−C) = 58 kcal/mol.[8a] This is also reflected by the calculated reaction enthalpies, which follow the same order: ΔE (kcal/mol) = 35.8 ($TiMe_4$),[17] 47.1 ($ZrMe_4$), and 58.8 ($HfMe_4$)[30] (see Figure 2 and Table 1, entries 2 and 8). These calculated high activation barriers and large endothermicities of the unimolecular mechanism of methane elimination from MMe_4 do not agree with observed instabilities of these

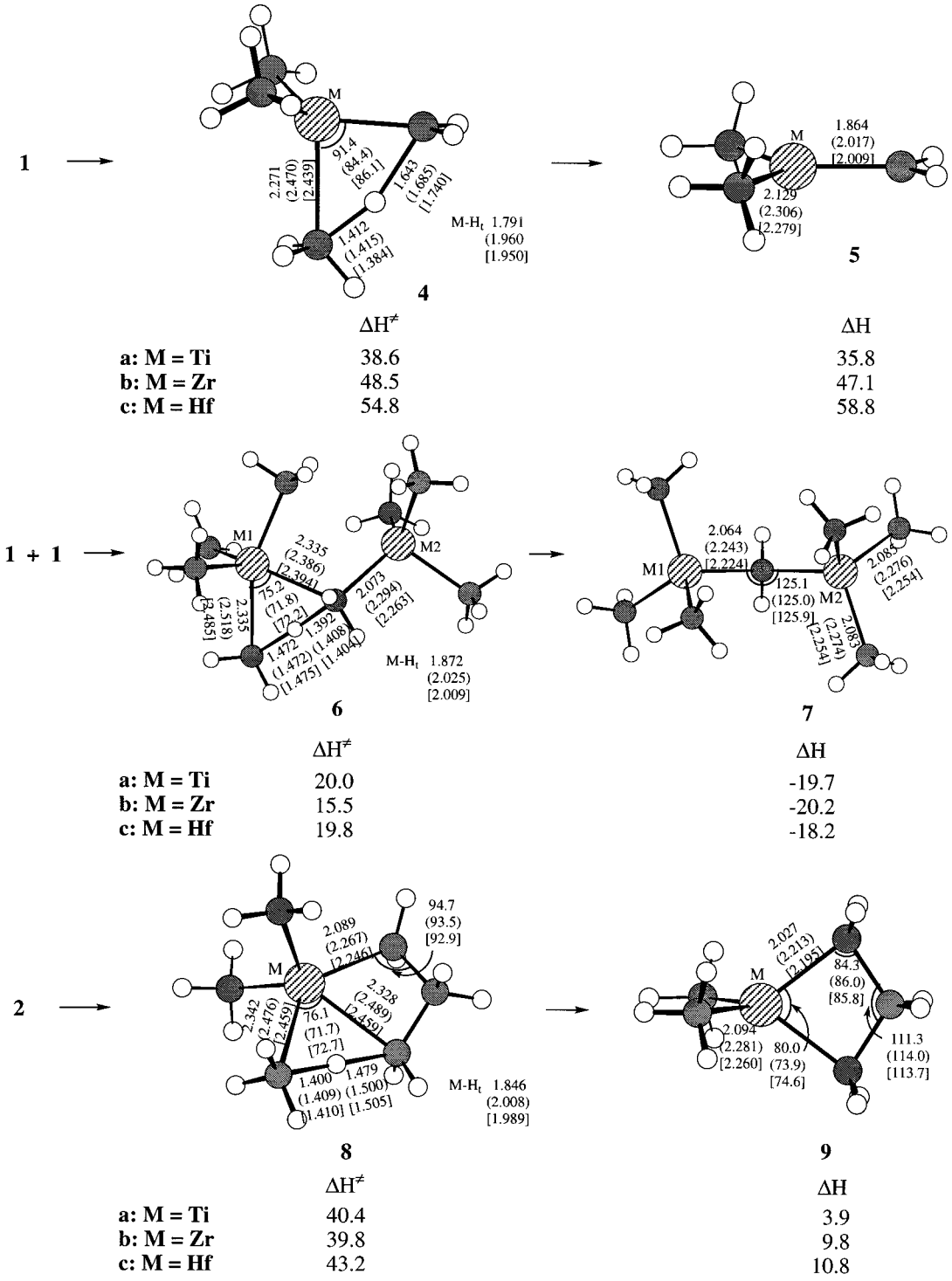

Figure 2. Calculated structures of transition states (**4**, **6**, **8**) and products (**5**, **7**, **9**) for monomeric α-H abstraction, dimeric α-H abstraction for MMe_4, and γ-H abstraction for M(n-Pr)Me_3 with the MP2/HW3 activation or reaction enthalpies (kcal/mol). Selected geometrical parameters calculated with the HF/HW3 method are given for M = Ti (**a**), Zr (**b**, in parentheses), and Hf (**c**, in brackets).

compounds, and the unimolecular mechanism can thus be ruled out.

(2) Bimolecular α-Hydrogen Abstraction of MMe_4. As in the titanium system, two transition structures (syn and anti, see ref 17 for the definition) have been located for the bimolecular methane elimination for MMe_4 (M = Zr, Hf), but only the more stable anti transition structure (**6**) is shown in Figure 2. The basic features of the transition structures for $ZrMe_4$ (**6b**) and $HfMe_4$ (**6c**) are very similar to those of $TiMe_4$ (**6a**). Contrary to the unimolecular mechanism, the calculated activation enthalpies are in the order $ZrMe_4$ (15.5 kcal/mol) < $HfMe_4$ (19.8 kcal/mol) < $TiMe_4$ (20 kcal/mol). How do we understand this? Two factors are operating in these transition structures. On one hand, the relative reactivity should reflect the relative M−C bond strength, just like the unimolecular mechanism; on the other hand, the bimolecular transition structures are destabilized by the steric interactions between the two molecules and by the formation of a pentacoordinated

metal center. Since the Ti−C bonds are about 0.2 Å shorter than the Zr−C and Hf−C bonds, the transition structure for $TiMe_4$ (**6a**) is much more crowded than those for $ZrMe_4$ (**6b**) and $HfMe_4$ (**6c**). This results in the highest activation barrier for $TiMe_4$. However, the Zr−C and Hf−C bond lengths are nearly identical, and $ZrMe_4$ is more reactive than $HfMe_4$ because the Zr−C bond is weaker.

The substantial decrease in the activation energy of the bimolecular mechanism for all three MMe_4 complexes is due to the formation of the M−C−M bridging moiety in the transition structure.[16,17] This is reflected by the calculated reaction energies that are quite exothermic for all three reactions (Figure 2 and Table 1, entries 4 and 10). Although these bimolecular reactions have quite large negative activation entropies (Table 1), they should still be much more favorable than the unimolecular reactions in solution.[17] In addition, the calculated activation energies for the bimolecular reactions indicate that $TiMe_4$ is more stable than $ZrMe_4$. This is in agreement with experiments. We conclude that MMe_4 complexes thermolyze through a bimolecular first reaction step.

(3) The γ-Hydrogen Abstraction of M(n-Pr)Me$_3$. The basic features of the located transition structures for Zr(n-Pr)Me_3 (**8b**) and Hf(n-Pr)Me_3 (**8c**) are similar to those of the titanium system (**8a**)[17] except that the Zr−C and Hf−C bond lengths are longer than the Ti−C bond lengths by about 0.15−0.2 Å on average. The two partially formed C−H bond lengths are also quite similar in these transition structures.[17] Thus, the C−M−C angles (71.7° for Zr and 72.6° for Hf) are slightly smaller than those of the titanium system (76°).[17]

The calculated activation enthalpies are 39.8 and 43.2 kcal/mol for Zr(n-Pr)Me_3 **(8b)** and Hf(n-Pr)Me_3 (**8c**) (see Figure 2 and Table 1, entries 5 and 11), respectively, which are lower than those of the α-hydrogen abstraction of $ZrMe_4$ (**4b**) and $HfMe_4$ (**4c**) by about 8.7 and 11.6 kcal/mol. This is quite interesting because, in the titanium case, we found that the activation energy for γ-hydrogen abstraction of Ti(n-Pr)Me_3 (**8a**) is higher than the α-hydrogen abstraction of $TiMe_4$ (**4a**) by about 2.2 kcal/mol (Figure 2).[17] These transition structures of γ-hydrogen abstraction are similar to those of bimolecular α-hydrogen abstraction, except that a four-membered metallacyclobutane ring is introduced. This four-membered ring causes significant destabilization because of ring strain. Thus, the M−C−C angles are changed from 117° in **2** to about 93−94° in **8**. Therefore, the calculated activation energies for these γ-hydrogen abstraction reactions are still quite high. The trend of activation energies for **8a**−**c** is also similar to that for **6a**−**c**, except that the energy difference between **8a** and **8b** is smaller than that between **6a** and **6b**. This is understandable because the steric interactions between the alkyl groups on the two metal centers destabilize **6a** more than **6b**, and these interactions are absent in transition structure **8**.

As expected, the difference in activation enthalpies between **8a**−**c** and **6a**−**c** parallel the difference in the reaction energies very well. We also note that the ring strain in the four-membered ring is somewhat larger in **9b** and **9c** than in **9a**. This is indicated by the smaller C−M−C angle (by about 6°) and larger C−C−C angle (by about 3°) in **9b** and **9c**.

C. Thermolysis Reaction of MNp$_4$. Experimental studies have indicated that MNp_4 (M = Ti, Zr, Hf) thermolyzes with first-order kinetics.[3b,12,18] Therefore, only unimolecular mechanisms were calculated in the present study. Figure 3 shows the calculated geometries of transition structures (**10**, **12**) and products (**11**, **13**) of the α-hydrogen and γ-hydrogen abstraction reactions for MNp_4 (M = Ti, Zr). The activation and reaction enthalpies shown in Figure 3 were calculated based on those of MP2/HW3 energetics of MMe_4 and M(n-Pr)Me_3 systems with correction of the steric interactions caused by the *tert*-butyl groups which were calculated with the HF/3-21G method (see note in Table 1).

As in MMe_4 and M(n-Pr)Me_3 systems, the basic features of the two transition structures for the $ZrNp_4$ system (**10b**, **12b**) are similar to those of $TiNp_4$ (**10a**, **10a**) except that the Zr−C bond lengths are longer than the Ti−C by about 0.15 Å.[31] Because of the release of the steric interactions introduced by the neopentyl groups, the calculated activation energy of the α-hydrogen abstraction for $ZrNp_4$ is reduced by about 5.3 kcal/mol compared with that of unimolecular α-hydrogen abstraction for $ZrMe_4$ with the HF/3-21G method (see Table 1, entries 1 and 13), and the activation energy of γ-hydrogen abstraction for $ZrNp_4$ is reduced by about 2.9 kcal/mol compared with that of Zr(n-Pr)Me_3 (see Table 1, entries 5 and 14). In titanium systems, the corresponding decreases of activation energies are 8.4 kcal/mol for α-hydrogen abstraction and 2.8 kcal/mol for the γ-hydrogen abstraction. The fact that α-hydrogen abstraction of $TiNp_4$ benefits more from the release of steric interaction than that of $ZrNp_4$ can be attributed to the more crowded environment in the reactant $TiNp_4$ because of the shorter Ti−C bond length. However, there are still severe steric interactions in the γ-hydrogen abstraction transition structures, so the decreases of activation energies for γ-hydrogen abstractions are almost the same for both titanium and zirconium systems.

As indicated above, the introduction of the bulky neopentyl groups favors the α-hydrogen abstraction process in both titanium and zirconium systems. In the titanium system, the activation energy for the unimolecular α-hydrogen abstraction for $TiMe_4$ is lower than the γ-hydrogen abstraction of Ti(n-Pr)Me_3 by about 2.4 kcal/mol. The preference for α-hydrogen abstraction is thus even larger in $TiNp_4$, about 7.8 kcal/mol with the MP2/HW3 level. However, the activation energy for the unimolecular α-hydrogen abstraction for $ZrMe_4$ is higher than the γ-hydrogen abstraction of Zr(n-Pr)Me_3 by about 8.2 kcal/mol. There is thus a large intrinsic preference for γ-hydrogen abstraction in the zirconium system. Therefore, the γ-hydrogen abstraction of $ZrNp_4$ is still more favorable than α-hydrogen abstraction, by about 5.2 kcal/mol with the MP2/HW3 level. Thus, for CVD of Zr−C from $ZrNp_4$, we predict that the first reaction step is through the γ-hydrogen abstraction instead of the α-hydrogen abstraction, which is different from $TiNp_4$.

Although calculations for $HfNp_4$ have not been carried out, qualitative prediction can be derived in comparison with $ZrNp_4$. Since the Hf−C and Zr−C bonds are nearly

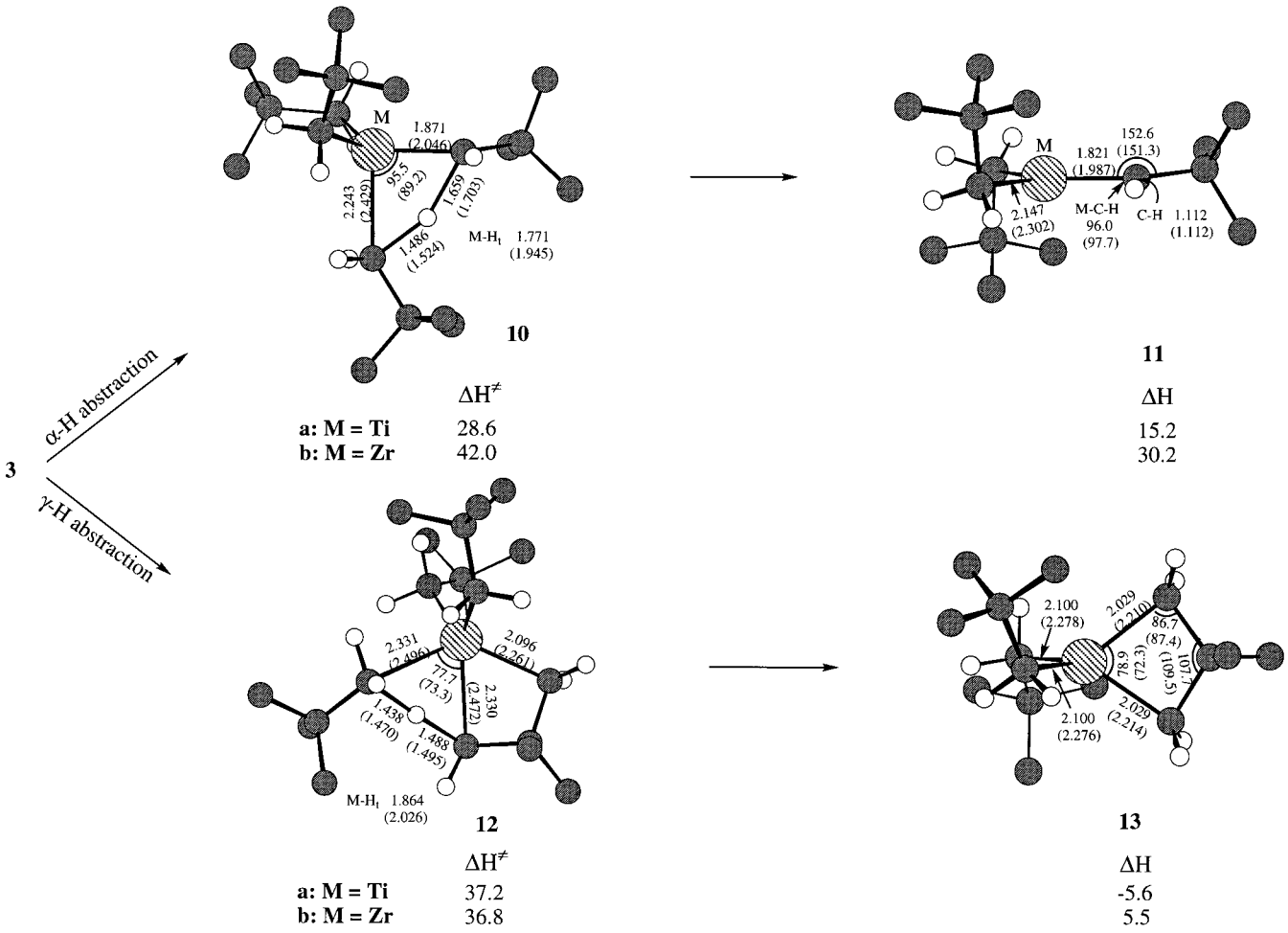

Figure 3. Calculated structures of transition states (**10**, **12**) and products (**11**, **13**) for the α-H and γ-H abstractions for MNp_4 with the MP2/HW3 activation and reaction enthalpies (kcal/mol). Selected geometrical parameters calculated with the HF/3-21G method are given for M = Ti (**a**), Zr (**b**, in parentheses). Methyl hydrogens are omitted for clarity.

the same, we expect very similar steric effects for the two systems. Therefore, unimolecular α-hydrogen abstraction for $HfNp_4$ would be about 6 kcal/mol higher in activation energy than that of $ZrNp_4$. On the other hand, the calculated activation energy for the γ-hydrogen abstraction of Hf(n-Pr)Me_3 is about 3.4 kcal/mol higher than that of Zr(n-Pr)Me_3. Therefore, we predict that compared with $ZrNp_4$, $HfNp_4$ has a higher preference for γ-hydrogen abstraction over α-hydrogen abstraction, and the latter decomposes slower.

The alkylidene product of the α-hydrogen abstraction (**11b**) is similar to its titanium analogue (**11a**) with a large Zr=C−C angle (151.3°) and small Zr=C−H angle (97.7°),[32] which indicates the α-agostic interaction of the α C−H bond.[28] The zirconacyclobutane product (**13b**) is slightly puckered with a dihedral angle C−C−Ti−C of about 12°, while its titanium analogue (**13a**) is essentially planar. This is due to the more crowded environment in the zirconacyclobutane (see above).

D. Experimental Studies of the Thermolysis of $ZrNp_4$ in the CVD of ZrC. The results of these ab initio calculations on the decomposition of Np_4Zr and the prediction that γ-hydrogen abstraction is preferred in this decomposition prompted us to study the decomposition experimentally. $Zr(CH_2CMe_3)_4$ ($ZrNp_4$-d_0) and $Zr(CD_2CMe_3)_4$ ($ZrNp_4$-d_8) were prepared from ZrX_4 (X = Cl, Br) and Me_3CCH_2Li or Me_3CCD_2MgBr and purified by sublimation. They were then used in chemical vapor decomposition (CVD) (400−500 °C, base pressure ca. 10^{-4}−10^{-5} Torr) similar to that reported by Smith and co-workers.[4a] The volatile products were collected in a liquid nitrogen trap and vacuum-transferred to a J. Young valved NMR tube.

The volatiles from the CVD with $ZrNp_4$-d_0 were analyzed by ^1H and ^{13}C NMR and found to be mainly neopentane and isobutene. By NMR, 2.3(0.4) mol of neopentane and 1.0(0.1) mol of isobutene are produced per mole of $ZrNp_4$. Neopentane and isobutene account for 82(4)% of the mass released in the formation of ZrC from $ZrNp_4$-d_0. The molar ratio of neopentane/isobutene in these volatiles was found to be 2.32(0.13) [or 69.9-(1.2)% neopentane vs 30.1(1.2)% isobutene].

The volatiles from the CVD with $ZrNp_4$-d_8 were analyzed by field-ionization mass spectrometry (FI-MS) and NMR. Previous reports[33] have shown that field ionization in FI-MS provides the parent peak of neopentane and reduces the fragmentation of neopentane to *tert*-butyl ions. In contrast, such fragmentation is essentially 100% in electron-impact mass spectrometry

(32) Several conformations for the bulky neopentyl groups were studied, and those shown in **10** and **12** were most stable.

(33) (a) Hindennach, P.; Block, J. *Ber. Bunsen-Ges. Phys. Chem.* **1971**, *75*, 993. (b) Tenschert, G.; Beckey, H. D. *Int. J. Mass Spectrom. Ion Phys.* **1971**, *7*, 97.

Table 2. Mass Spectra (*m/e* = 72−75) Generated upon 6 kV Ionization of the Volatiles of the CVD with $(Bu^tCD_2)_4Zr$

m/e	relative intensity[a,32]
72	26.1
73	24.9
74	100
75	25.3

[a] All peaks are normalized to give the strongest peak an intensity of 100.

(EI-MS).[3b] The intensities of the peaks at mass 72−75 by FI-MS are shown in Table 2. An analysis of these peaks shows the following distribution of neopentane isotopologues: 15% d_0, 14% d_1, 59% d_2, 12% d_3.[34] Neopentane-d_2, $(H_3C)_3C-CHD_2$, was also observed in the $^{13}C\{^1H\}$ NMR spectrum; $-CHD_2$ as a 1:2:3:2:1 quintet was identified at 31.21 ppm (isotopic shift $^1\Delta$: +0.60 ppm). The ratio of neopentane-d_2/neopentane-d_3 from FI-MS is 4.9. This ratio is much higher than that (0.57) observed in the thermal decomposition of $TiNp_4$-d_8 under CVD conditions.[3b]

Two possible pathways are consistent with the formation of the large amount of neopentane-d_2: γ-hydrogen abstraction and a radical mechanism (to form $Np_3Zr^\bullet$ and $Np^\bullet$); in contrast, α-hydrogen abstraction predicts that the predominant neopentane isotopologue should be neopentane-d_3. A GC/MS analysis showed there was no dineopentyl (2,2,5,5-tetramethylhexane), a possible product of $Np^\bullet$ dimerization, in the volatiles from the CVD with $ZrNp_4$-d_8. The lack of dineopentyl may not rule out the radical mechanism. However, it suggests that the radical mechanism is unlikely the major pathway. The large amount of neopentane-d_2 formed and the lack of dineopentyl suggest, as predicted by the ab initio calculations, that γ-hydrogen abstraction is likely to be the major thermal decomposition pathway. The formation of neopentanes-d_0 and -d_1 indicates that other processes occur in the CVD with $ZrNp_4$-d_8. These processes perhaps occur later in the decomposition sequence,[35] as close to 3 mol of neopentane are formed per mole of $ZrNp_4$. Neopentanes-d_0 and -d_1 were observed in the thermolysis of $TiNp_4$-d_8 as well and were attributed to unknown processes likely occurring later in the thermolysis sequence.[3c]

A GC/MS analysis of the volatiles from the CVD with $ZrNp_4$-d_8 showed the presence of both isobutene-d_0 and -d_2.[36] The NMR of the volatiles from the CVD with $ZrNp_4$-d_8 is also consistent with the presence of both isobutene-d_0 and isobutene-d_2 $(CH_3)_2C{=}CD_2$ (see Experimental Section). The presence of isobutene-d_1 $(CH_3)_2C{=}CHD$ is unlikely, as it is not seen in either ^1H (in the $=CHD$ region) or $^{13}C\{^1H\}$ NMR.[36] The molar ratio of isobutene-d_2/isobutene-d_0 was obtained from ^1H NMR and was found to be 1.52(0.1). The percentage of neopentane-d_0, -d_1, -d_2, and -d_3 was then used in the analysis of the ^1H NMR spectra to give the molar ratio 2.38(0.12) of neopentane/isobutene [or 70.4(1.1)% neopentane vs 29.6(1.1)% isobutene] in the sample. It is interesting to note that this molar ratio in the volatiles from CVD with $ZrNp_4$-d_8 is about the same as that [2.32(0.13) or 69.9(1.2)% neopentane vs 30.1(1.2)% isobutene] in the volatiles from the CVD with $ZrNp_4$-d_0. These observations suggest that both $Zr(CH_2CMe_3)_4$ and $Zr(CD_2CMe_3)_4$ follow similar pathways in their thermal decomposition and are consistent with the prediction by ab initio calculations that γ-hydrogen abstraction is preferred in their decomposition.

How to explain the observed ratio of about 1.5 for isobutene-d_2/isobutene-d_0? These species are presumably produced from the [2+2] ring opening of metallocyclobutane (**A**),[37] the product of the γ-hydrogen abstraction reaction, as shown in Scheme 2. Our effort to locate a transition structure for the ring-opening reaction was unsuccessful due to a high endothermicity. The reaction occurs in the gas phase because of a large reaction entropy. We expect that the transition structure of the reaction is very late and is close to the reaction product. Therefore, the kinetic isotope effect should be similar to product isotope effect. Model calculations for the ethene elimination from $Me_2Ti(CH_2CH_2CD_2)$ using the density functional theory B3LYP/6-311G** method[38] (the 6-311G** basis set is not available for Zr atom) indicated a 1.5-fold preference for the formation of ethene-d_2.[39] Such a large secondary product isotope effect is due to the fact that the alkylidene C−H bond is close to a normal $C_{sp^3}-H$ bond. Thus, the deuterium atoms favorably go to ethene where they form stronger bonds with the sp^2 carbon atom.

Scheme 2

$$ZrNp_4\text{-}d_8 \rightarrow Np_2ZrCD_2CMe_2CH_2\ (\mathbf{A}) + NpH\text{-}d_2$$

$$(\mathbf{A}) \rightarrow Np_2ZrCH_2 + Np_2ZrCD_2 + CH_2{=}CMe_2 + CD_2{=}CMe_2$$

E. Summary. Quantum mechanics calculations have been carried out for the unimolecular and bimolecular methane elimination from MMe_4, methane elimination from M(n-Pr)Me_3 through γ-hydrogen abstraction (M = Ti, Zr, Hf), and neopentane elimination from MNp_4 (M = Ti, Zr) through α-hydrogen and γ-hydrogen abstractions. The results are summarized as follows: (1) The activation energy for the unimolecular methane elimination for MMe_4 increases in the order $TiMe_4 \ll ZrMe_4 < HfMe_4$. The calculated activation energies for the systems are so high that the mechanism can be excluded. (2) The MMe_4 are predicted to thermolyze through the bimolecular mechanism with the reactivity $ZrMe_4 > HfMe_4 > TiMe_4$. This is in agreement with experimentally observed reactivities. (3) In agreement

(34) In obtaining the ratios of the neopentane isotopologues, corrections were made for (1) the M − 1 peaks (Experimental Section) and (2) natural abundance ^{13}C isotopologues.

(35) It is not clear if surface reactions lead to the formation of these neopentane isotopologues.

(36) The isotopologues of isobutenes were not separated by the GC/EI-MS. The EI-MS spectrum of isobutene-d_2 $(CH_3)_2C{=}CD_2$ would overlap with those of isobutene-d_0 and isobutene-d_1 $(CH_3)_2C{=}CHD$. The M − 1 and M − 2 peaks of isobutene-d_2 $(CH_3)_2C{=}CD_2$ will overlap with those of parent $(CH_3)_2C{=}CDH$ and $(CH_3)_2C{=}CH_2$, respectively. Isobutene-d_0 was identified in the difference MS spectrum. See: Derrick, P. J.; Burlingame, A. L. *J. Am. Chem. Soc.* **1974**, *96*, 4909, for the MS of isobutene isotopologues.

(37) (a) Rappe, A. K.; Goddard, W. A. *J. Am. Chem. Soc.* **1982**, *104*, 448. (b) Anslyn, E. V.; Grubbs, R. H. *J. Am. Chem. Soc.* **1987**, *109*, 4880.

(38) (a) Lee, C.; Yang, W.; Parr, R. G. *Phys. Rev. B* **1988**, *37*, 785. (b) Beck, A. E. *J. Chem. Phys.* **1993**, *98*, 5648.

(39) We are grateful to Professor M. Saunders of Yale University for his kindness in allowing us to use the Quiver Program with which the isotope effect was calculated.

with experiments, $TiNp_4$ favors the α-hydrogen abstraction over γ-hydrogen abstraction, largely due to larger release of steric interactions in the former. (4) $ZrNp_4$ and $HfNp_4$ prefer γ-hydrogen abstraction over α-hydrogen abstraction. (5) The CVD of ZrC with $ZrNp_4$-d_0 and $ZrNp_4$-d_8 has been carried out. The analysis of volatile products reveals that about 2.3 mol of neopentane and 1 mol of isobutene are produced per mole of $ZrNp_4$. In the $ZrNp_4$-d_8 case, the ratio of NpH-d_2/NpH-d_3 is about 4.9. These results are quite different from those in the CVD of TiC with $TiNp_4$-d_0 and $TiNp_4$-d_8 and strongly support the prediction that $ZrNp_4$ thermolyzes with the first step of γ-hydrogen abstraction.

Acknowledgment. We are grateful to the Hong Kong Research Grants Council for financial support of the work (Y.D.W.). Z.X. thanks the US NSF Young Investigator Award (NYI) program (Grant CHE-9457368), the DuPont Young Professor Award, the Camille Dreyfus Teacher-Scholar Award, and the State of Tennessee Science Alliance program for the financial support of this research.

Supporting Information Available: Calculated energy, thermal energy and entropy, and Cartesian coordinates of species involved in the thermolysis of MMe_4, MMe_3(n-Pr) (M = Zr, Hf), and $ZrNp_4$. This material is available free of charge via the Internet at http://pubs.acs.org.

OM980595V